ISSN 1682-296X (Print) ISSN 1682-2978 (Online)

Bio Technology



ANSImet

Asian Network for Scientific Information 308 Lasani Town, Sargodha Road, Faisalabad - Pakistan



RESEARCH ARTICLE OPEN ACCESS

DOI: 10.3923/biotech.2015.109.118

Effect of DksA Protein on the Susceptibility of *Escherichia coli* Towards Novel Amine N-Halamine Polymeric Nanoparticles as Powerful Antibiotics

¹Qigeqi Dong, ¹Lifei Fan, ²Alideertu Dong and ¹Morigen ¹College of life Science, Inner Mongolia University, Hohhot, 010021, People's Republic of China ²College of Chemistry and Chemical Engineering, Inner Mongolia University, Hohhot, 010021, People's Republic of China

ARTICLE INFO

Article History:

Received: December 29, 2014 Accepted: March 30, 2015

Corresponding Author:
Alideertu Dong,
College of Chemistry and Chemical
Engineering,
Inner Mongolia University,
Hohhot, 010021,
People's Republic of China

ABSTRACT

A novel amine N-halamine polymeric nanoparticles (ANHP NPs) based on 4-(allyloxy)-2,2,6,6-tetramethylpiperidine (ATMP) were well developed as an antimicrobial agents by the aid of the radical copolymerization for deactivating pathogenic bacteria. The as-prepared ANHP NPs were systematically characterized by the different physical and chemical techniques like ¹H NMR, FTIR, SEM and the modified iodometric/thiosulfate method. Sterilizing action of the ANHP NPs on bacterial strain was evaluated by selecting different types of *Escherichia coli* (*E. coli*) strains as model microorganisms. The effect of DksA protein on the susceptibility of *E. coli* towards the ANHP NPs was investigated via the plate counting technique and the zone of inhibition test. The experimental results showed that DksA protein has an excellent resistance against the ANHP NPs. Such an in-depth study on the DksA effect on the susceptibility of *E. coli* against the antibiotics opens up a new thought for us to develop the novel potential antibiotics.

Key words: N-halamine nanoparticles, antibacterial, DksA protein, susceptibility, *Escherichia coli*

INTRODUCTION

Bacterial infection is one of the most common causes of the increasing lethal diseases (Ditommaso et al., 2014; Feliciano et al., 2014; Iranmanesh et al., 2014). The pathogen contamination is the root of many persistent bacterial infections (Chaudhry et al., 2014). A rising numbers of antibacterial agents with potent capability of combating with pathogen bacteria were thus drastically developed (Carmona-Ribeiro and Carrasco, 2013; Choi et al., 2013; Xiao et al., 2013; Kumar et al., 2010; Munoz-Bonilla et al., 2013). Investigation into the antibacterial action induced by the N-halamine type biocides actually represents one of the most explored research fields in the world of antibiotic applications (Badrossamay and Sun, 2008, 2009; Zhao and Liu, 2011; Liu and Sun, 2006; Zhao et al., 2011). Behind their exceptional bactericidal property, what make the N-halamines fascinating are their inherent

advantages such as good stability for long-term use, storage over a wide temperature range, ability to be regenerated in a chlorine solution repeatedly, lack of corrosion, low toxicities and relatively low expense (Li *et al.*, 2013). Therefore, the N-halamines are considered as the promising tools in the future development of effective antibacterial materials.

Antimicrobial action of the N-halamines is based on the transfer of positive oxidative halogen from the N-halamines to bacterial cells (Hui and Debiemme-Chouvy, 2013; Kenawy *et al.*, 2007). The oxidative halogen possesses a strong tendency to kill bacteria. As reported previously, bactericidal activity of the N-halamines is tightly related to their activated surface area (Zhao *et al.*, 2014). The N-halamines with larger surface area can give more antibacterial functional sites to combat bacteria as a result showing enhanced biocidal efficiency. Thereby, nano-sized N-halamines could appear more overwhelming bactericidal

activity over their bulk powder counterparts which has been proven repeatedly in our previous reports (Dong *et al.*, 2010, 2011a-c, 2013, 2014a, b). Stability is another decisive factor determining the antibacterial activity and even the subsequent applications of N-halamines (Barnes *et al.*, 2006). N-halamines can be composed of one or more imide/amide/amine N-halamine bond and their stability is in an order of amine>amide>imide N-halamine (Gutman *et al.*, 2014). Thus, the development of stable amine type N-halamines has attracted increasing attention, yet there is limited report recently.

Escherichia coli as one of the typical human pathogen bacteria, is widely selected as model bacteria for evaluating the antibacterial activity of the biocides (Cui et al., 2012; Kong and Jang, 2008; Wang and Lim, 2013). Many proteins or factors are involved in all kinds of cell damage repair for adaptive survival responses. In absence of these proteins or factors, cell damage would occur which could result in a wide range of functional disturbance and even cell death if not restored in due course. Kang and Craig (1990) reported a new kind of gene in E. coli, DksA (dnaK suppressor gene, maps at 3.7 min on the E. coli chromosome) which could encode the DksA protein. When chromosome breaks occur at two or more locations in E. coli chromosome, DksA interacted with RecN would study by displacing RNAP from the DNA template at replication-transcription collisions to repair double-strand breaks (DSBs) and to restart subsequent replication (Meddows et al., 2005).

Although, the repair function of DksA protein on DNA double strand breaks has been well known, the effect of DksA protein on the susceptibility of E. coli towards the antibiotics has been ill-defined. In this study, we well discussed the susceptibility of E. coli on faced with N-halamines in the presence and absence of DksA protein. We developed a novel amine N-halamine polymeric NPs (ANHP NPs) as potent biocides form 4-(allyloxy)-2, 2, 6, 6-tetramethylpiperidine (ATMP) through the modification of poly (methyl methacrylate) (PMMA) nanoparticles with amine N-halamine. The photo and chemical structure of the ANHP NPs are shown in Fig. 1. The the formation of the ANHP NPs were success characterized by the different techniques such as Fourier transform infrared (FTIR), Nuclear Magnetic Resonance (NMR), Scanning Electron Microscopy (SEM) and the modified iodometric/thiosulfate titration. In order to evaluate the bactericidal capability, E. coli with different types of strains were selected as model bacteria. The as-synthesized ANHP NPs have powerful bactericidal activity against E. coli. Furthermore, the effect of DksA protein on the sensitivity of E. coli towards the ANHP NPs was investigated as well. In light of such an in-depth study, it would be valuable of clarifying the role of DksA and even extending the industrial application of the amine N-halamines.



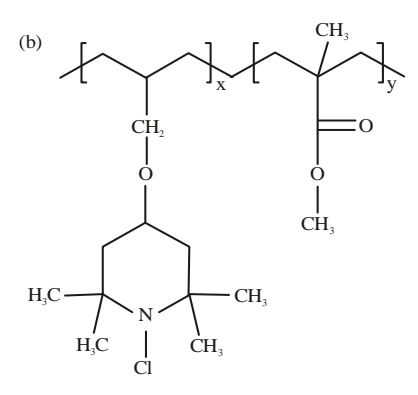


Fig. 1(a-b): (a) Photo and (b) Chemical structure of the ANHP NPs

MATERIALS AND METHODS

Materials: Anhydrous ethanol, Tetrahydrofuran and petroleum ether were available from Beijing Chemical Company. Methyl methacrylate, potassium persulfate and magnesium sulfate were purchased from Tianjin Chemical Reagent Plant and Shanghai Chemical Reagent Plant, respectively. The 2, 2, 6, 6-Tetramethyl-4-piperidinol (TMP) was provided by Nangong Shenghua Chemicals Co., Ltd. Allyl bromide and sodium hypochlorite were obtained from Sinopharm Chemical Reagent Co., Ltd. Sodium hydride was purchased from Beijing Hengye Zhongyuan Chemical Co., Ltd.

Synthesis of ANHP Nps: The preparation of the ANHP NPs was performed via a three-step process. Typically, 3.97 g of 2, 2, 6, 6-tetramethyl-4-piperidinol (TMP) was added in a sealed flask with 50 mL of THF and then stirred under a nitrogen atmosphere at ambient temperature. About 0.66 g of NaH was poured into the flask and stirred for 30 min. The 2.4 mL of allyl bromide was added dropwise in the mixture and stirred for 30 min at ambient temperature and then for 12 h at 65°C under a nitrogen atmosphere. The byproduct sodium bromide was removed by filtration and the THF solvent by distillation. The crude product was added in 50 mL of ultrapure water and the mixture was extracted with 50 mL

of petroleum ether. The organic phase was dried over anhydrous MgSO₄ and the solvent was removed by distillation to give the pure ATMP (Hui and Debiemme-Chouvy, 2013). Secondly, a mixture of 0.1 g of ATMP dissolved in 3 mL of MMA was added into 100 mL of ultrapure water containing 0.1 g of potassium persulfate with a condenser and a N₂ gas inlet. The reaction mixture was maintained at 75°C with vigorous stirring to obtain the poly(ATMP-co-MMA) NPs (Dong *et al.*, 2011a). Finally, 0.5 g of the Poly (ATMP-co-MMA) NPs were immersed in 150 mL commercial sodium hypochlorite solution (10 wt. %) and stirred at room temperature. The as-prepared ANHP NPs were washed thoroughly with a mixture of water and ethanol and then dried at 40°C for 24 h to remove any remaining free chlorine from the surface of the sample (Dong *et al.*, 2014a).

Determination of oxidative chlorine content: Oxidative chlorine content of the ANHP NPs was determined by the modified iodometric/thiosulfate titration procedure (Dong *et al.*, 2014a). The percentage of active chlorine (Cl %) for the sample was calculated according to the following equation (Dong *et al.*, 2014a).

Cl (%) =
$$\frac{35.5}{2} \times \frac{(V_{Cl} - V_0) \times 10^{-3} \times 0.01}{W_{Cl}} \times 100$$

where, V_{Cl} and V_0 are the volumes (mL) of sodium thiosulfate solutions consumed in the titration of the chlorinated and unchlorinated samples, respectively and W_{Cl} is the weight of the chlorinated sample (g).

Characterization: FTIR spectra were captured by using a Thermo Nicolet (Woburn, MA) Avatar 370 FTIR spectrometer using KBr pellet method in the range of 400-4000 cm⁻¹ to analyze the sample compositions. The transmittance mode at a resolution of 4 cm⁻¹ by averaging 32 scans was utilized. ¹H NMR spectra were recorded on a Bruker AVANCE-500 NMR spectrometer in DMSO solution and the chemical shift values were given in parts per million (ppm). The morphology, particle size, surface state, size distribution and elemental mapping of the samples were observed on a Shimadzu SSX-550 field emission Scanning Electron Microscope (SEM) at 15.0 kV. The samples were dispersed in ethanol with assistance of sonication and casted onto the silicon wafer for SEM and then dried at room temperature before examination.

Bacterial strains and culture: In the plate counting experiment, *Escherichia coli* BW25113 (wildtype) and derivatives strains were used as summarized in Table 1. BW25113 was wildtype strain in *E. coli*. As for MOR1050, DksA gene was replaced by cat from BW25113 chromosome by one step inactivation method. The *phoP* gene was replaced by cat by the same method in MOR302 as a negative control. The neo is kanamycin resistant gene, cat is chromophenicol resistant gene. Cells were grown at 37°C and samples taken

Table 1: Strains used in this study

Strains	Relevant genotype	Reference	
BW25113	Wild-type	Baba et al. (2006)	
MOR1050	BW25113∆DksA::cat	This study	
MOR302	BW25113∆phoP::neo	Baba et al. (2006)	

until optical density $OD_{600} = 0.8$ for Luria Bertani (LB) medium with shaking at 180 rpm. The 1 mL of bacterial liquid with 10^0 was taken and dilute until 10^{-3} . Then $10~\mu L$ of bacteria liquid from the 10^{-3} mixing was taken twice into two EP tubes, respectively, one was for experimental group while the other for control. The $90~\mu L$ of different concentration of the ANHP NPs was added with well contacting for 1 h, then add $900~\mu L$ of $Na_2S_2O_3$ solution to neutralize the active chlorine and stop the antibacterial action. The same procedure was carried out for the control test by replacing the ANHP NPs with sterilized water. The mixture was spread onto LB plates for overnight culture, cell sensitivity for the ANHP NPs was detected by colony counting.

The inhibition zone study of the ANHLS NPs was carried out by a modified Kirby-Bauer technique. Thirty microliter of bacteria liquid from the 10^{-3} mixing was taken into two EP tubes respectively, adding 970 μL of sterilized water into both tubes. The mixture was spread onto the surface of LB agar plate. The plates were then allowed to stand at room temperature for 1 min. The ANHLS NPs were placed onto the surface of the bacteria-containing agar plate and gently pressed with a sterile forceps to ensure full contact between the sample and the agar. After incubation overnight at 37°C, the inhibition zone around the sample was measured.

RESULTS AND DISCUSSION

Characterization of the ANHP Nps: The products ANHP NPs were evidenced by recognizing the characteristic groups using FTIR technique as shown in Fig. 2a. The spectrum shows strong C-H characteristic peak at around 2930 and 2980 cm⁻¹ which are an effective evidence for -CH₂- group reflecting the formation of the polymeric carbon framework (Sun et al., 2010). A strong band at about 1735 cm⁻¹ as a structural label for C = O group is ascribed to the ester group of the MMA structural component in polymers (Wang et al., 2013a). Additionally, the C-N and N-Cl characteristic peak appeared at around 1230 and 750 cm⁻¹, respectively (Chen and Sun, 2006). The multiplet of C-O-C stretching is detected within the range of 1070-1170 cm⁻¹ regarding to the ether bond from ATMP units in polymers (Wang et al., 2013b). The presence of C-N, C-O-C and N-Cl vibration can act as marker for the formation of the ATMP structural units in polymer chains. Besides, almost invisible N-H stretching vibration appeared at about 3435 cm⁻¹ (Sun et al., 2010). Most of N-H bonds have been transformed to N-Cl groups and this weak N-H peak is likely corresponding to the un-chlorinated amine group inside the NPs. A broad peak around 3500 cm⁻¹ is attributed to the stretching vibration of O-H group possibly

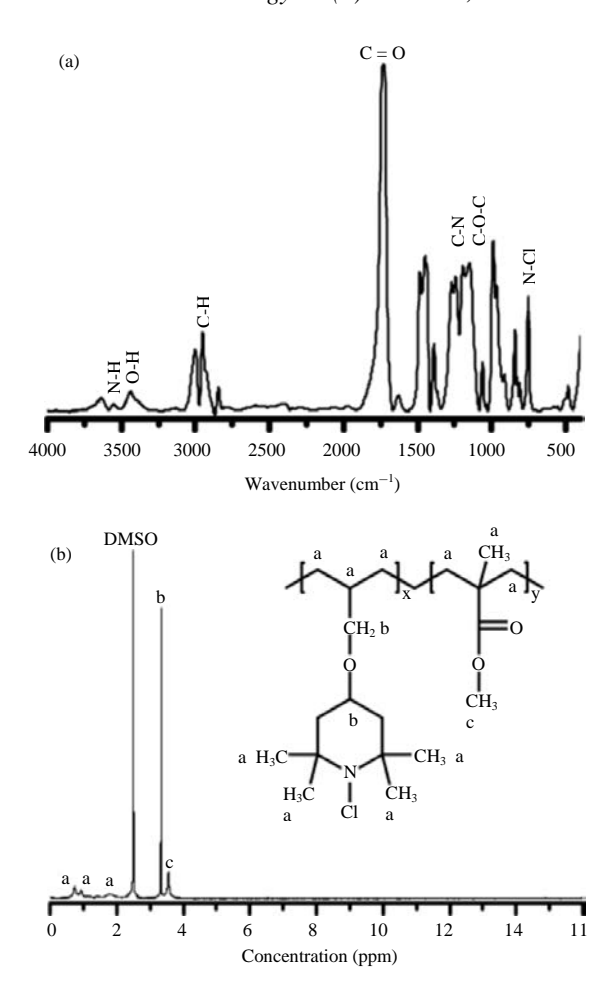


Fig. 2(a-b): (a) FTIR and (b) ¹H NMR spectrum of the ANHP NPs

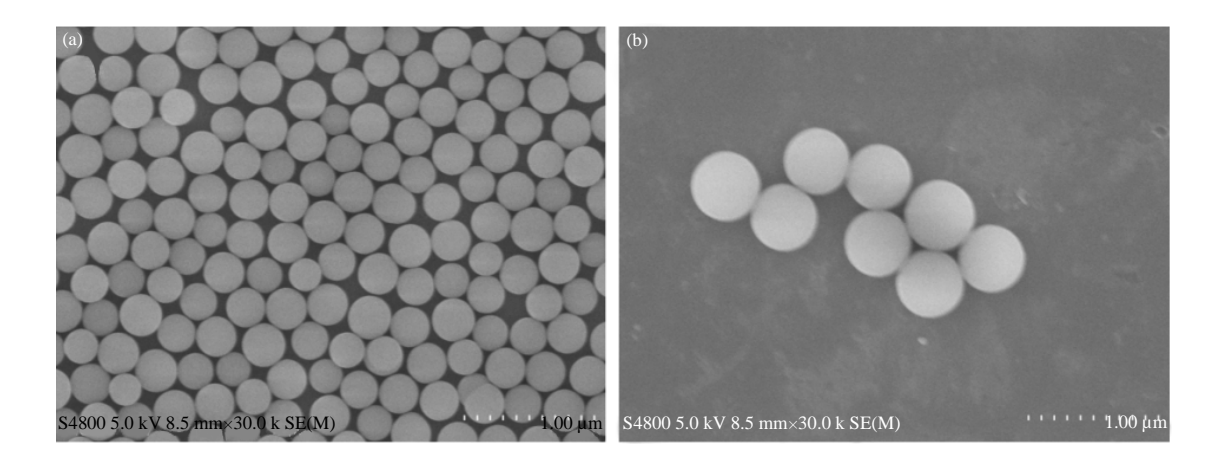
from the residual water (Liu *et al.*, 2012a, b; Pu *et al.*, 2009). The existence of these vibrations well confirmed the success of the ANHP NPs.

To further verify the product, 1H NMR of the ANHP NPs is given in Fig. 2b. A strong characteristic fitting peak for solvent DMSO is found at $\delta = 2.5$ ppm (Lu *et al.*, 2010). In the lower ppm region $\delta < 2.0$ ppm, the characteristic signals for -CH₂- units of the polymer chain are densely distributed, suggesting that the as-prepared ANHP NPs have relative longer carbon chain and higher molecular weight. Besides, the characteristic signals for -CH₃ group of ATMP and MMA component are also detected in this region. The assignments of the strong signals at $\delta = 3.3$ ppm is corresponding to -CH₂- and >CH- group of ATMP structural component. As for MMA component, O-CH₃ group shows signals at $\delta = 3.8$ ppm. The integration of the >CH- and O-CH₃ group well confirmed the formation of the ANHP NPs which is in well agreement with FTIR results.

In order to capture morphological and structural information of the ANHP NPs, SEM technique was employed. For comparison, the pure poly(methyl methacrylate) nanoparticles (PMMA NPs) were fabricated by the same

method as control materials and the corresponding SEM analysis was carried out as well. Figure 3a and b give the representative SEM image of the ANHP NPs (A) and pure PMMA NPs (B). The ANHP NPs are uniform, quasi-monodisperse, spherical and smooth, showing flawless surface without any cracks or degradation. There is no significant difference between the ANHP NPs and PMMA NPs in morphology, structure, shape and surface state from SEM image. From such a result, we can easily conclude that the introducing ATMP component almost has no subversive effect on the appearance of the ANHP NPs.

However, these two products show the different particle size and size distribution. For veracity, more than 200 particles were selected from SEM image for each product to measure the diameter and the average particle size and size distribution were calculated. The particle size and size distribution results of the ANHP NPs and PMMA NPs are illustrated in Fig. 3c and d, respectively. It is visible obviously that the ANHP NPs have a smaller size versus the larger sized PMMA NPs. The mean particles size of the ANHP NPs and PMMA NPs is 296.3 and 529.7 nm, respectively. Thus it can be concluded that ATMP could reduce particle size possibly



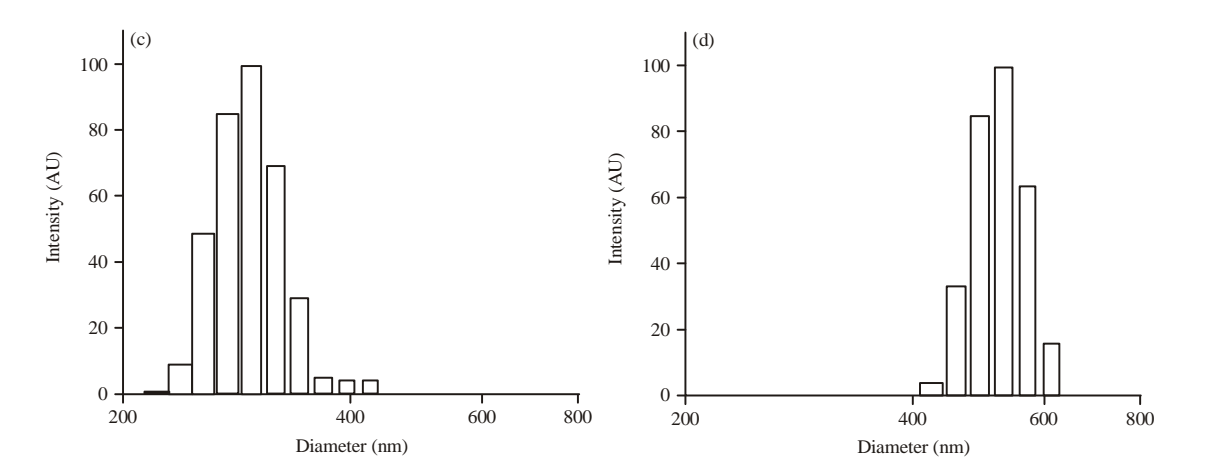


Fig. 3(a-d): (a, b) TEM and (c, d) Particle size distribution of the (a, c) ANHP NPs and the (b, d) Pure PMMA NPs

due to the nature of allylic structure. As reported previously, it is difficult to synthesis the required ATMP homopolymer with high molecular weight through the radical polymerization because of its autoinhibition action from allyl group (Jang and Kim, 2008). In this study, MMA with the ester group was introduced as comonomer to copolymerize with ATMP which is favourable to the radical polymerization as a result enhance the chain propagation reaction of ATMP during the radical polymerization process to achieve the required product with desired molecular weight (Jang and Kim, 2008). This is the reason why we chose MMA in this study. The ANHP NPs possess wider size distribution ranged from 210-440 nm, whereas the sizes of the PMMA NPs are in the region of 430-620 nm showing narrow distribution. Such a distribution widening phenomenon of the ANHP NPs is may be owing to the disruption induced by introducing ATMP in the original MMA homopolymerization system. The difference in reaction activity between two monomers during radical polymerization is another plausible explanation. The MMA is more active than ATMP towards chain propagation reaction which lead to heterogeneous polymerization showing wide size distribution.

As expected, the antimicrobial behavior of the N-halamines is mainly dependent on N-H-N-Cl transformation (Padmanabhuni et al., 2012). The N-halamines kill bacteria via the transfer of oxidative halogen from N-halamines biocides to bacterial cells, resulting in the inhibition or even destruction of bacterial metabolic processes. As mentioned above, physical techniques like FTIR, NMR and SEM analyses well proved the N-H-N-Cl transformation. Besides, the formation of the ANHP NPs was further validated by a chemical oxidation-reduction reaction, the iodometric/thiosulfate method (Luo et al., 2006). Two oxidation-reduction reactions were performed in the iodometric/thiosulfate method as shown in Fig. 4a. In order to verify these two reactions, the color changes involved in the iodometric/thiosulfate method were photographed Fig. 4b. Each of the color plates detected from the photographs is corresponding to the product of the oxidation-reduction reactions. In Fig. 4b, the ANHP NPs were completely dispersed in aqueous solution by the aid of the sonication, showing transparent solution. After adding the KI and H₂SO₄, the oxidative chlorine in the ANHP NPs solution oxidize (a) $N-Cl+2I^-+H^+ = N-H+I_2+Cl^-$

 $\begin{array}{c} I_{2} + 2S_{2}O_{3}^{2} - 2I + S_{4}O_{6}^{2} - \\ \\ (e) \\ \\ \end{array}$

Fig. 4(a-e): (a) Oxidation-reduction reactions and (b-e) The photographs of the color changes involved in the iodometric/thiosulfate titration

immediately iodide ions to produce yellow colored iodine as Fig. 4c. This solution turn to dark blue by adding starch in Fig. 4d, further evidencing the existence of the iodine. The as-produced iodine then can be exhausted by the added thiosulfate for color fading, showing almost complete transparent solution in Fig. 4e. Such a color change well confirmed the success of the two oxidation-reduction reactions and more importantly the N-H→N-Cl transformation was further authenticated.

Antibacterial evaluation of the ANHP Nps: The as-synthesized products, ANHP NPs, can be utilized as bactericides for treating microorganism. For investigation, bacterial suspension was herein selected as simulated water polluted by pathogenic bacteria for testing bactericidal activity of the ANHP NPs. The antibacterial performance of the ANHP NPs was examined against model bacteria *E. coli* by using the

plate counting method (Ghosh *et al.*, 2012). Figure 5 shows photographs of the bacterial LB culture plates, visualizing the survival case of *E. coli* after 60 min exposure to the control and the ANHP NPs. Survival of *E. coli* colonies on the LB culture plates was seen as small white dots. The control plate shows dense bacterial colonies. On contrary, the population reduction of the bacterial colonies is visible after contacting with the ANHP NPs which demonstrates the excellent antimicrobial activity of the ANHP NPs towards *E. coli*. We believe that such a powerful antibacterial activity of the ANHP NPs is competitive enough to those reported previously (Dong *et al.*, 2010, 2011a-c, 2013, 2014a, b).

In order to investigate the role of DksA, we constructed the DksA deletion mutant strain via replacing DksA with *cat* by one step inactivation method (Datsenko and Wanner, 2000) from *E. coli* wildtype strain BW25113, named as MOR1050. The phoP deletion mutant strain (MOR302 which is the

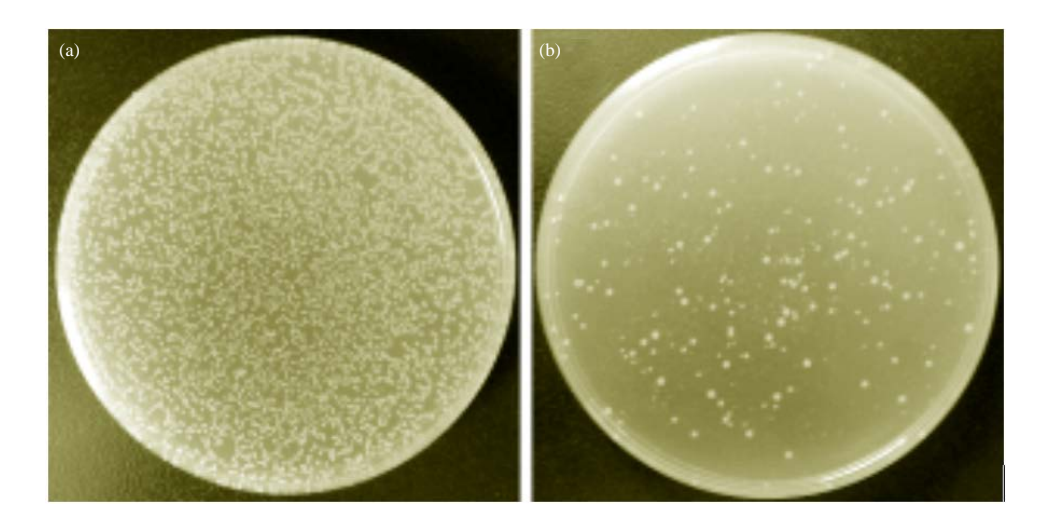


Fig. 5(a-b): Bacterial culture plates of E. coli upon a 60 min contacting with the (a) Control and (b) ANHP NPs

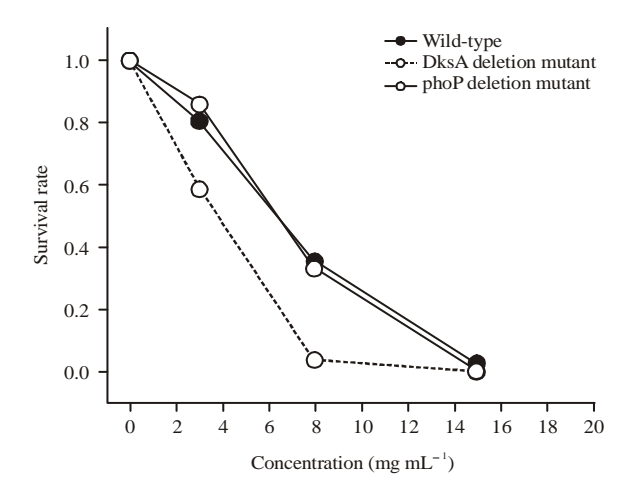


Fig. 6: Survival rate of wildtype, DksA deletion mutant and phoP deletion mutant in *E. coli* towards the ANHP NPs with different concentrations

Table 2: Survival rate of the different strains towards the ANHP NPs with different concentrations

Strains	Relevant genotype	ANHP NPs (mg mL $^{-1}$)	Survival rate (Mean±SD)	Reference
BW25113	Wild-type	3.0	0.804 ± 0.152	Baba et al. (2006)
MOR1050	BW25113ΔDksA::cat		0.585±0.135	This study
MOR302	BW25113∆phoP::neo		0.858 ± 0.053	Baba et al. (2006)
BW25113	Wild-type	8.0	0.354 ± 0.231	Baba et al. (2006)
MOR1050	BW25113∆DksA::cat		0.038 ± 0.022	This study
MOR302	BW25113ΔphoP::neo		0.333±0.041	Baba et al. (2006)
BW25113	Wild-type	15.0	0.028 ± 0.022	Baba et al. (2006)
MOR1050	BW25113∆DksA::cat		0.000 ± 0.000	This study
MOR302	BW25113∆phoP::neo		0.005±0.002	Baba et al. (2006)

member of the two-component regulatory system phoQ/phoP involved in adaptation to low Mg²⁺ environments) was also used as a negative control as shown in Table 1 (Baba *et al.*, 2006). To determine whether DksA protein was involved in cell protection, a plate counting method was utilized under the different ANHP NPs concentrations (0, 3.0, 8.0 and 15.0 mg mL⁻¹) as illustrated in Fig. 6. The detailed data is

summarized in Table 2. The comparison of the susceptibility between the ANHP NPs treated cells and the control shows that the DksA deletion mutant strain expresses increased sensitivity to the ANHP NPs in comparison with wildtype while the negative control, phoP deletion mutant strain, has no significant difference with wildtype. With the increased concentration of the ANHP NPs, the DksA deletion mutant

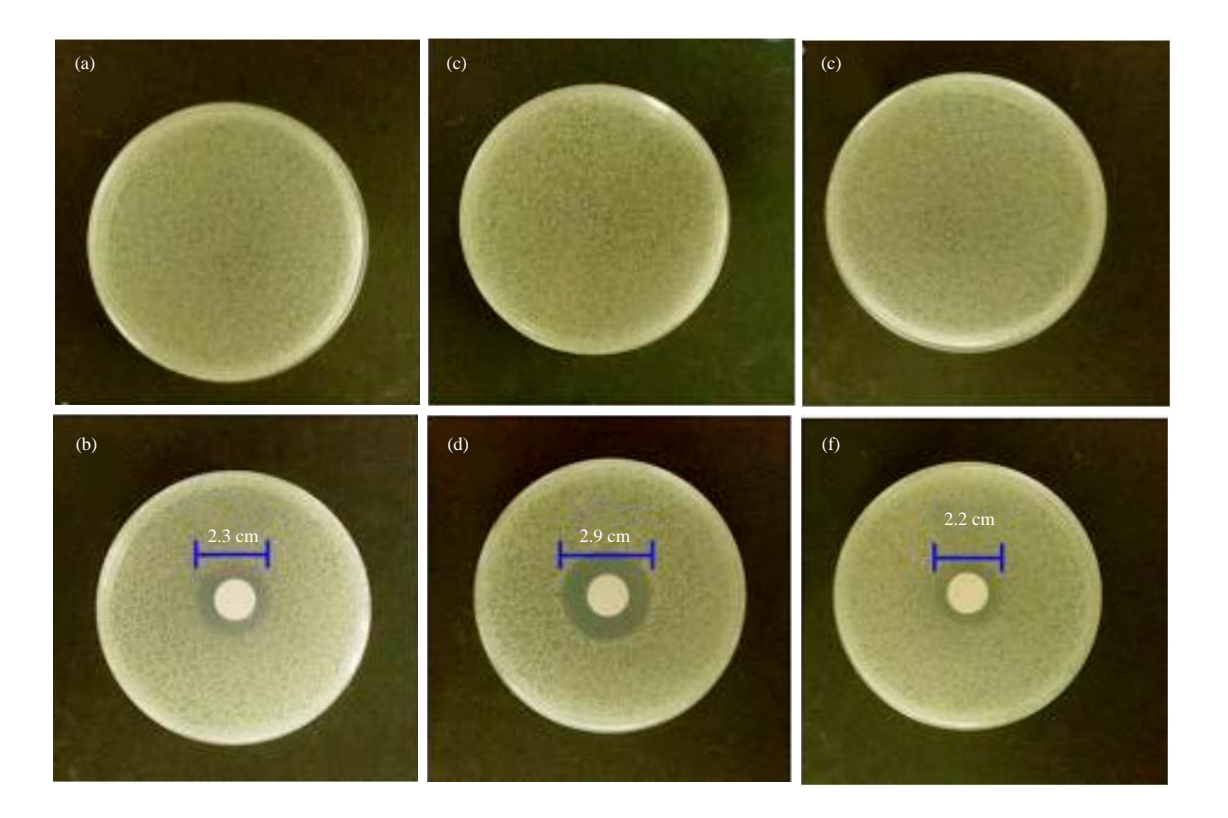


Fig. 7(a-f): Optical images of the zone of inhibition against (a, b) Wildtype, (c, d) DksA deletion mutant and (e, f) PhoP deletion mutant in *E. coli* for the control (upper) and the ANHP NPs (down)

strain displayed more sensitivity in comparison with wildtype and the negative control. Increasing the concentration of the ANHP NPs from 0-15.0 mg mL⁻¹, the survival rate of cell immediately decreased when DksA was absent while survival rate of cells were decreased much slowly when DksA was present. As the concentration reached to 15.0 mg mL⁻¹, there was no survival colonies detected for DksA deletion mutant strain, revealing high fragility on faced with higher concentration of the ANHP NPs. Such a result suggests that the DksA was involved in cell protection against the ANHP NPs.

Effect of DksA on the sensitivity of *E. coli* towards the ANHP NPs was further assessed using the zone of inhibition study as shown in Fig. 7. The ANHP NPs were processed into small disc and *E. coli* with different strains (wildtype and two derivatives strains) were selected as experimental microorganism. The inhibition zone reflects the susceptibility of the bacteria towards the biocides, i.e., the wider the inhibition zone is, the higher susceptibility it will represent (Sun *et al.*, 2012). The ANHP NPs provide an apparent inhibition zone with diameter of 2.3 cm for wildtype, 2.9 cm for DksA deletion mutant and 2.2 cm for phoP deletion mutant in *E. coli*. It was clearly shown that the inhibition zone was larger for DksA deletion mutant strain than those of the wildtype and phoP deletion mutant. That is to say, the DksA

was involved in cell protection against the ANHP NPs which is in well agreement with the result shown in plate counting method.

CONCLUSION

In conclusion, we developed a simple approach for the design and synthesis of amine N-halamine polymeric nanoparticles (ANHP NPs) based on 2, 2, 6, 6-tetramethyl-4piperidinol via the radical copolymerization for deactivating pathogenic bacteria. The success of the ANHP NPs was confirmed by the different physical and chemical techniques such as ¹H NMR, FTIR, SEM and the iodometric/thiosulfate method. Different types of Escherichia coli strains were chosen as model microorganisms to prove the sterilizing action of the ANHP NPs on bacterial strain. Antibacterial assay prove that the ANHP NPs possess superior bactericidal activity against E. coli. By using the plate counting technique and the zone of inhibition measurement, the effect of DksA protein on the susceptibility of E. coli towards the ANHP NPs was well established, i.e., DksA protein has an excellent resistance against the ANHP NPs. This in-depth study provides us a new possibility for developing the novel potential antibiotics.

ACKNOWLEDGMENT

The study was supported by grant from the National Natural Science Foundation of China "NSFC" (Grant No. 31360208 to Morigen); the Natural Science Foundation of Inner Mongolia (Grant No. 20102009 to Morigen) and the Program of Higher-level Talent of Inner Mongolia University "SPH-IMU" (Grant No. Z20090107 to Morigen).

REFERENCES

- Baba, T., T. Ara, M. Hasegawa, Y. Takai and Y. Okumura et al., 2006. Construction of Escherichia coli K-12 in-frame, single-gene knockout mutants: The Keio collection. Mol. Syst. Biol., Vol. 2. 10.1038/msb4100050
- Badrossamay, M.R. and G. Sun, 2008. Acyclic halamine polypropylene polymer: Effect of monomer structure on grafting efficiency, stability and biocidal activities. React. Funct. Polym., 68: 1636-1645.
- Badrossamay, M.R. and G. Sun, 2009. A study on melt grafting of N-halamine moieties onto polyethylene and their antibacterial activities. Macromolecules, 42: 1948-1954.
- Barnes, K., J. Liang, R. Wu, S.D. Worley, J. Lee, R.M. Broughton and T.S. Huang, 2006. Synthesis and antimicrobial applications of 5, 5'-ethylenebis [5-methyl-3-(3-triethoxysilylpropyl) hydantoin]. Biomaterials, 27: 4825-4830.
- Carmona-Ribeiro, A.M. and L.D.D.M. Carrasco, 2013. Cationic antimicrobial polymers and their assemblies. Int. J. Mol. Sci., 14: 9906-9946.
- Chaudhry, W.N., I.U. Haq, S. Andleeb and I. Qadri, 2014. Characterization of a virulent bacteriophage LK1 specific for *Citrobacter freundii* isolated from sewage water. J. Basic Microbiol., 54: 531-541.
- Chen, Z. and Y. Sun, 2006. N-halamine-based antimicrobial additives for polymers: Preparation, characterization and antimicrobial activity. Ind. Eng. Chem. Res., 45: 2634-2640.
- Choi, J.B., J.S. Park, M.S. Khil, H.J. Gwon and Y.M. Lim *et al.*, 2013. Characterization and antimicrobial property of poly (acrylic acid) nanogel containing silver particle prepared by electron beam. Int. J. Mol. Sci., 14: 11011-11023.
- Cui, J., C. Hu, Y. Yang, Y. Wu and L. Yang *et al.*, 2012. Facile fabrication of carbonaceous nanospheres loaded with silver nanoparticles as antibacterial materials. J. Mater. Chem., 22: 8121-8126.
- Datsenko, K.A. and B.L. Wanner, 2000. One-step inactivation of chromosomal genes in *Escherichia coli* K-12 using PCR products. Proc. Natl. Acad. Sci. USA., 97: 6640-6645.
- Ditommaso, S., M. Giacomuzzi, S.R.A. Rivera and C.M. Zotti, 2014. Does better identification of the *Legionella pneumophila* serogroup 1 strains by Sequence-Based Typing (SBT) allow for the implementation of more effective contamination control strategies and more targeted intervention measures? Microchem. J., 115: 126-129.

- Dong, A., Q. Zhang, T. Wang, W. Wang, F. Liu and G. Gao, 2010. Immobilization of cyclic N-halamine on polystyrene-functionalized silica nanoparticles: Synthesis, characterization and biocidal activity. J. Phys. Chem. C, 114: 17298-17303.
- Dong, A., J. Huang, S. Lan, T. Wang and L. Xiao et al., 2011a. Synthesis of N-halamine-functionalized silicapolymer core-shell nanoparticles and their enhanced antibacterial activity. Nanotechnology, Vol. 22. 10.1088/0957-4484/22/29/295602
- Dong, A., S. Lan, J.F. Huang, T. Wang and T.Y. Zhao *et al.*, 2011b. Modifying Fe₃O₄-functionalized nanoparticles with N-halamine and their magnetic/antibacterial properties. Applied Mater. Interfaces, 3: 4228-4235.
- Dong, A., S. Lan, J.F. Huang, T. Wang and T.Y. Zhao *et al.*, 2011c. Preparation of magnetically separable N-halamine nanocomposites for the improved antibacterial application. J. Colloid Interface Sci., 364: 333-340.
- Dong, A., Y. Sun, S. Lan, Q. Wang and Q. Cai *et al.*, 2013. Barbituric acid-based magnetic N-halamine nanoparticles as recyclable antibacterial agents. ACS Applied Mater. Interfaces, 5: 8125-8133.
- Dong, A., M. Xue, S. Lan, Q. Wang and Y. Zhao *et al.*, 2014a. Bactericidal evaluation of N-halamine-functionalized silica nanoparticles based on barbituric acid. Colloids Surf. B: Biointerfaces, 113: 450-457.
- Dong, A., Z. Huang, S. Lan, Q. Wang and S. Bao *et al.*, 2014b. N-halamine-decorated polystyrene nanoparticles based on 5-allylbarbituric acid: From controllable fabrication to bactericidal evaluation. J. Colloid Interface Sci., 413: 92-99.
- Feliciano, C.P., Z.M. de Guzman, L.M.M. Tolentino, M.L.C. Cobar and G.B. Abrera, 2014. Radiation-treated Ready-To-Eat (RTE) chicken breast *Adobo* for immunocompromised patients. Food Chem., 163: 142-146.
- Ghosh, S., V.S. Goudar, K.G. Padmalekha, S.V. Bhat, S.S. Indi and H.N. Vasan, 2012. ZnO/Ag nanohybrid: Synthesis, characterization, synergistic antibacterial activity and its mechanism. RSC Adv., 2: 930-940.
- Gutman, O., M. Natan, E. Banin and S. Margel, 2014. Characterization and antibacterial properties of N-halamine-derivatized cross-linked polymethacrylamide nanoparticles. Biomaterials, 35: 5079-5087.
- Hui, F. and C. Debiemme-Chouvy, 2013. Antimicrobial N-halamine polymers and coatings: A review of their synthesis, characterization and applications. Biomacromolecules, 14: 585-601.
- Iranmanesh, M., H. Ezzatpanah and N. Mojgani, 2014. Antibacterial activity and cholesterol assimilation of lactic acid bacteria isolated from traditional Iranian dairy products. LWT-Food Sci. Technol., 58: 355-359.
- Jang, J. and Y. Kim, 2008. Fabrication of monodisperse silica-polymer core-shell nanoparticles with excellent antimicrobial efficacy. Chem. Commun., 2008: 4016-4018.

- Kang, P.J. and E.A. Craig, 1990. Identification and characterization of a new *Escherichia coli* gene that is a dosage-dependent suppressor of a dnaK deletion mutation. J. Bacteriol., 172: 2055-2064.
- Kenawy, E.R., S.D. Worley and R. Broughton, 2007. The chemistry and applications of antimicrobial polymers: A state-of-the-art review. Biomacromolecules, 8: 1359-1384.
- Kong, H. and J. Jang, 2008. Antibacterial properties of novel poly (methyl methacrylate) nanofiber containing silver nanoparticles. Langmuir, 24: 2051-2056.
- Kumar, A.S., S. Sornambikai, L. Deepikab and J.M. Zenc, 2010. Highly selective immobilization of amoxicillin antibiotic on carbon nanotube modified electrodes and its antibacterial activity. J. Mater. Chem., 20: 10152-10158.
- Li, R., P. Hu, X.H. Ren, S.D. Worley and T.S. Huang, 2013. Antimicrobial N-halamine modified chitosan films. Carbohydr. Polym., 92: 534-539.
- Liu, B., W. Zhang, Q. Zhang, H. Zhang, J. Yu and X. Yang, 2012a. Facile method for synthesis of hollow porous magnetic microspheres with controllable structure. J. Colloid Interface Sci., 375: 70-77.
- Liu, H., D. Wang and X. Yang, 2012b. Preparation of polymer at titania raspberry-like core-corona composite via heterocoagulated self-assembly based on hydrogenbonding interaction. Colloids Surf. A: Physicochem. Eng. Aspects, 397: 48-58.
- Liu, S. and G. Sun, 2006. Durable and regenerable biocidal polymers: Acyclic N-halamine cotton cellulose. Ind. Eng. Chem. Res., 45: 6477-6482.
- Lu, H., B. Xu, Y. Dong, F. Chen and Y. Li *et al.*, 2010. Novel fluorescent pH sensors and a biological probe based on anthracene derivatives with aggregation-induced emission characteristics. Langmuir, 26: 6838-6844.
- Luo, J., Z. Chen and Y. Sun, 2006. Controlling biofilm formation with an N-halamine-based polymeric additive. J. Biomed. Mater. Res. Part A, 77: 823-831.
- Meddows, T.R., A.P. Savory, J.I. Grove, T. Moore and R.G. Lloyd, 2005. RecN protein and transcription factor DksA combine to promote faithful recombinational repair of DNA double-strand breaks. Mol. Microbiol., 57: 97-110.
- Munoz-Bonilla, A., M.L. Cerrada, M. Fernandez-Garcia, A. Kubacka, M. Ferrera and M. Fernandez-Garcia, 2013. Biodegradable polycaprolactone-titania nanocomposites: Preparation, characterization and antimicrobial properties. Int. J. Mol. Sci., 14: 9249-9266.

- Padmanabhuni, R.V., J. Luo, Z. Cao and Y. Sun, 2012. Preparation and characterization of N-halamine-based antimicrobial fillers. Ind. Eng. Chem. Res., 51: 5148-5156.
- Pu, H., X. Zhang, J. Yuan and Z. Yang, 2009. A facile method for the fabrication of vinyl functionalized hollow silica spheres. J. Colloid Interface Sci., 331: 389-393.
- Sun, X., Z. Cao, N. Porteous and Y. Sun, 2010. Amine, melamine and amide N-halamines as antimicrobial additives for polymers. Ind. Eng. Chem. Res., 49: 11206-11213.
- Sun, X., Z. Cao, N. Porteous and Y. Sun, 2012. An N-halamine-based rechargeable antimicrobial and biofilm controlling polyurethane. Acta Biomaterialia, 8: 1498-1506.
- Wang, W., X. Wang, Q. Yang, X. Fei, M. Sun and Y. Song, 2013a. A reusable nanofibrous film chemosensor for highly selective and sensitive optical signaling of Cu²⁺ in aqueous media. Chem. Commun., 49: 4833-4835.
- Wang, W., Y. Zhang, Q. Yang, M. Sun and X. Fei *et al.*, 2013b. Fluorescent and colorimetric magnetic microspheres as nanosensors for Hg²⁺ in aqueous solution prepared by a sol-gel grafting reaction and host-guest interaction. Nanoscale, 5: 4958-4965.
- Wang, X. and T.T. Lim, 2013. Highly efficient and stable Ag-AgBr/TiO₂ composites for destruction of *Escherichia coli* under visible light irradiation. Water Res., 47: 4148-4158.
- Xiao, L.H., T. Wang, T.Y. Zhao, X. Zheng and L.Y. Sun et al., 2013. Fabrication of magneticantimicrobial-fluorescent multifunctional hybrid microspheres and their properties. Int. J. Mol. Sci., 14: 7391-7404.
- Zhao, L., X. Yan, Z. Jie, H. Yang, S. Yang and J. Liang, 2014.
 Regenerable antimicrobial N-halamine/silica hybrid nanoparticles. J. Nanopart. Res., Vol. 16. 10.1007/s11051-014-2454-7
- Zhao, N. and S. Liu, 2011. Thermoplastic semi-IPN of polypropylene (PP) and polymeric N-halamine for efficient and durable antibacterial activity. Eur. Polym. J., 47: 1654-1663.
- Zhao, N., G.G. Zhanel and S. Liu, 2011. Regenerability of antibacterial activity of interpenetrating polymeric Nhalamine and poly(ethylene terephthalate). J. Applied Polym. Sci., 120: 611-622.